EG UK Theory and Practice of Computer Graphics (2010)
John Collomosse, Ian Grimstead (Editors)

Craniofacial reconstruction based on skull-face models extracted from MRI datasets

M. Salas and S. Maddock

Department of Computer Science, University of Sheffield, UK

Email: {M.Salas | S.Maddock}@dcs.shef.ac.uk

Abstract

We present a method for extracting skull and face models from MRI datasets and show how the resulting dataset is used in a craniofacial reconstruction (CFR) system. Datasets for 60 individuals are used to produce a database of 3D skull-face models, which are then used to give faces to unknown skulls. In addition to the skull-face geometry, other information about the individuals is known and can be used to aid the reconstruction process. The results of the system were evaluated using different criteria providing the system with different combinations of age, gender, body build and geometric skull features. Based on a surface to surface distance metric, the real and estimated faces produced were compared using different head models from the database with a leave-one-out strategy. The reconstruction scores obtained with our CFR system were comparable in magnitude (average distance less than 2.0 mm) to other craniofacial reconstruction systems. The results suggest that it is possible to obtain acceptable face estimations in a CFR system based on skull-face information derived from MRI data.

1. Introduction

Craniofacial reconstruction techniques are used in forensic applications when other methods of identification cannot be applied [Evi00]. In these situations, a forensic artist using skull-face anthropometric data creates facial estimations based on her experience, the biological information deduced from the skull and other external sources of information such as *in situ* evidence. Usually, the data about the skull-face relation is based on anthropometric tables containing tissue depth measurements at a discrete set of points distributed in prominent areas of the skull and face. When manual reconstruction techniques are used, due to the subjectivity introduced by the artist and the limited information on the skull-face relation, the results are difficult to reproduce and evaluate. Computational techniques can also be used for producing face estimations. However, the results are limited when only anthropometric tables are used due to the amount and type of data available. Modern 3D scanning technologies, which are able to produce detailed data can be used to generate new information sources. We present a technique for creating accurate skull and face models from MRI data, and show the benefits of using these models in CFR.

Extracting the face layer is relatively straightforward for MRI data using the marching cubes isosurfacing technique [LC87], since only the border of the head volume needs to be identified. Extracting the skull is more difficult. Section 2 will describe previous attempts to do this and present our approach, which is based on a 3D deformation model guided by features in the MRI volume and statistical skull shape information. Section 3 will present the craniofacial reconstruction process that we have developed, based on the skull-face models extracted from the MRI datasets. Section 4 will present the results, with Section 5 presenting conclusions.

2. Skull extraction

MRI skull segmentation has been a research topic for several years [RBH*00, DSL05, MMB06]. Previous work has tried to conduct this segmentation process by considering homogeneity properties of bone regions. Assuming that skull voxels possess specific attributes allowing their classification in terms of intensity, colour, texture or movement, most of the approaches provide acceptable results only in certain areas of the head. Separability assumptions of tissue types are difficult to meet when presented with skull regions in MRI. The

DOI: 10.2312/LocalChapterEvents/TPCG/TPCG10/143-150

air and the skull voxels have practically no difference in intensity, colour or texture attributes. The only difference is the spatial position of each voxel relative to the global structure of the skull. Another property which makes the skull extraction process more difficult is the high intensity variation in regions of bone where fat concentration is high.

Mathematical Morphology, a method of image analysis used for extracting image components proves a quantitative description of geometrical structures. This method has been used for extracting the skull [DSL05]. In some regions of the skull (e.g. the upper part) these techniques provide acceptable results but fail in the frontal area.

Probabilistic approaches, which have been used successfully for classifying tissue types in medical images [CSB07, BA] have also been used for skull segmentation with similar results in the frontal area of the skull [DSL05]. With models of parameterised distributions for each type of tissue, they try to solve the partial volume problem in order to produce adequate voxel classifications [LMVS03, LFB98, HED*97].

Deformable models based methods guided by voxel intensities are another type of technique that have been used. The works of Rifai [RBH*00], Mang [MMB06], and Ghadimi [GAMK*08] are examples of these techniques. Again, these techniques rely on separability and regularity assumptions of the materials to segment. The method proposed by Shan [SHJ*07] for segmenting the skull combines CT and MRI in a registration approach. A set of skull models generated from CT segmentations is used for segmenting skull data in MRI modalities. The main drawback of combining CT and MRI technologies is that they require a number of CT scans in order to produce the initial skull models. CT scans produce a high radiation dose that can be harmful. Also the segmentation produced is simply a collection of isolated voxels that in a second stage have to be integrated to create a skull model. Based on several deformable skull templates defined at different resolutions, Luthi et. al. combine a deformable model approach with a shape restriction term generated from training skull shapes [LLA*08]. The results of each deformed model are combined to produce a segmentation. The approach requires several skull samples to make the skull shape term robust. In contrast, our method requires a unique initial deformable model and a small set of sampled skull shapes.

2.1. Our approach

In this research, a probabilistic method to approximate a 3D skull model from an MRI volume of the head is presented. The method uses a deformable model which iteratively adjusts its shape to fit the skull embedded in an MRI volume. Shape changes in the deformable model are defined combining two elements: information provided by the MRI volume and knowledge about the 3D structure of a skull shape. The influence of these two components is modelled as a Bayesian energy formulation:

$$E(M) = E_{volume}(f,V) + \Gamma E_{shape}(M) \tag{1}$$

where E is the energy provided by the deformable model M, V is the MRI volume, f is a set of features associated with the volume V, E_{volume} is an energy function of the features and E_{shape} is the energy contribution of the shape. The term E_{volume} is defined considering a 3D Gradient Vector Flow (GVF) field acting on the volume V. The shape term benefits contours that are more probable given the current spatial distribution of the control points even if they are far from the mean shape. Different and specialised training sets can be constructed to improve the statistical skull model (i.e. using heads models with similar skull proportions to the unknown skull). Both energies work together to find a solution. As the image feature is a function defined in terms of the gradient, it is maximised in the border region of the skull volume. The shape term is also a convergent function defined by the probability distribution of the training set. It is minimised when the configuration of the control points of the model corresponds to the data spanned by the distribution of probability. When combined, a trade-off between the shape and image features need to be established. The real segmentation result lies in the space between the two function extremes. In the current implementation the combination of both terms is controlled by the Γparameter.

A GVF for the field $v(x)$ is defined as the equilibrium solution for the vector diffusion equation [XP00]:

$$u_t = g(|\bigtriangledown f|)\bigtriangledown^2 u - h(|\bigtriangledown f|)(u - \bigtriangledown f) \tag{2a}$$

$$u(x,0) = \bigtriangledown f(x) \tag{2b}$$

The term $h(|\bigtriangledown f|)$ will produce a smoothly varying vector field. The term $(u - \bigtriangledown f)$ encourages a vector field u to be close to $\bigtriangledown f$ (gradient) computed from the data. The weighting functions g and h are used to control the influence of each term in the result. The shape term used in this research E_{shape} is defined as follows:

$$E_{shape}(s) = -\frac{1}{2}(s-\mu)^T \Sigma_{\perp}^{-1}(s-\mu) \tag{3}$$

In this equation, s is a shape descriptor of model M defined by a set of control points, μ is the average of the training set and $\Sigma_{\perp}$ is the regularised covariance matrix of the training set [Sal10]. The shape of the skull is modelled with a Gaussian distribution of control points associated with a skull model.

2.2. Alignment of Training Shapes

To conduct the statistical shape analysis of the skull it is necessary to provide a common reference system for the skull models to be compared. Taking the definition of shape given by D.G. Kendall [DM98] which states that "Shape is all the geometrical information that remains when location, scale and rotational effects are filtered out from an object", we

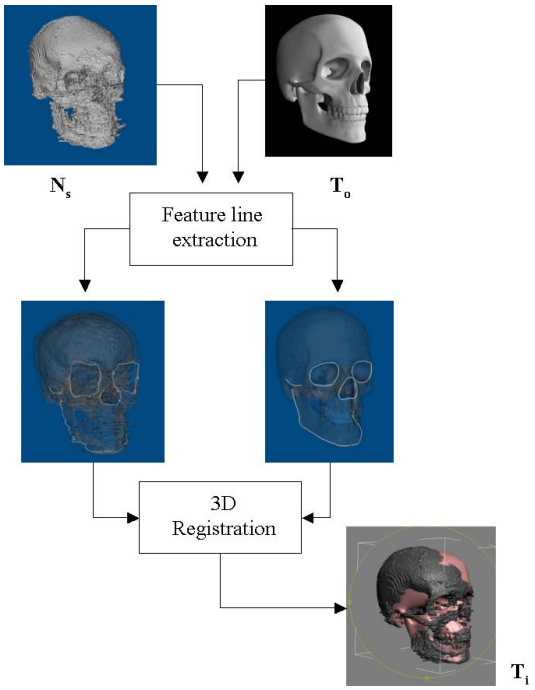

Figure 1: *Skull Template initialisation. A noisy skull approximation N_s is used to initialise the skull template model T_o by means of a registration step using a robust point match algorithm [CR]*

can achieve this by means of an alignment process on the skull models. Given a set of m training vectors $= \{s_i\}_{i=1..m}$ which are centered and normalised, we are interested in finding an optimal alignment for dealing with the scale and pose estimation of the shapes [DM98], [KBCL99]. An optimal alignment of two shapes s and $\hat{s}$ with respect to rotations, translation and scaling (known as full Procrustes fit [DM98]) requires the following distance to be minimsed:

$$D^2(s,\hat{s}) = \| \hat{s} - s\Gamma - 1_k\Gamma^T \|^2 \tag{4}$$

where D is the distance between the two shapes, $>= 0$ is a scaling factor, Γ is a rotation matrix, 1_k is a vector of ones (k x 1) vector, and Γa vector accounting for translations. Setting the corresponding derivatives to zero, the solution for the optimal parameters $\hat{}$, Γ, and$\hat{\Gamma}$ are the following expressions [KBCL99], [Sma96]:

$$\Gamma = 0 \tag{5}$$
$$\hat{\Gamma} = UV^T \tag{6}$$

The rotation term $\hat{\Gamma}$ is defined in terms of the matrices U and V derived from a single value decomposition of the matrix product $\frac{\hat{s}^T s}{\|s\|\|\hat{s}\|}$ as follows:

$$\frac{\hat{s}^T s}{\| s \| \| \hat{s} \|} = V\Lambda U^T \tag{7}$$

It can be shown that the best rotation estimator $\hat{}$ can be obtained by the following ratio [DM98]:

$$\hat{} = \frac{trace(\hat{s}^T s\hat{\Gamma})}{trace(s^T s)} \tag{8}$$

and finally, the expression defining the best alignment for the shape $\hat{s}$ is:

$$\hat{s} = \hat{} s_c\hat{\Gamma} + 1_k\Gamma^T + \sqrt{D^2(s_c,\hat{s})} \tag{9}$$

where s_c is the centered version of shape s. The energy can be minimised by applying the chain rule on the gradient descent equation:

$$\frac{ds}{dt} = -\frac{dE_{shape}(s)}{ds} = -\frac{dE_{shape}(\hat{s})}{d\hat{s}} \cdot \frac{d\hat{s}}{ds_c} \cdot \frac{ds_c}{ds} \tag{10}$$

with:

$$\frac{dE_{shape}(\hat{s})}{d\hat{s}} = (\Sigma_\perp^{-1}(s-\mu))^T \tag{11}$$

$$\frac{ds_c}{ds} = (I_{3n} - \frac{1}{n}\Gamma) \tag{12}$$

$$\frac{d\hat{s}}{ds_c} = \frac{d(\hat{} s_c\hat{\Gamma} + 1_k\Gamma^T + \sqrt{D^2(s_c,\hat{s})})}{ds_c} \tag{13}$$

The terms D, Γ,$\hat{\Gamma}$, and $\hat{}$ in equation 13 are all functions of the aligned shape $\hat{s}$ using the results of equations 4-8.

2.3. Deformable Model Algorithm

The algorithm to control the skull template evolution is shown in figure 2. It deforms the skull template to find a skull model that best fits the information provided by a skull volume approximation created in a pre-processing stage. In this stage the vector field associated to the initial skull volume is also produced. The initial skull volume is generated by a semiautomatic region growing process [LJZ03]. The initial noisy skull volume contains information about approximate proportions of the skull, position and orientation. The information is used to reduce the search space of the solution (see figure 1). The deformation is conducted by changing the positions of a set of control points defined in the deformable model according to the volume features and the shape restrictions. The stop condition used is a fixed number of iterations. At each iteration, the deformable model control points are moved towards the direction of the most probable skull configuration. The displacement of the control points is stored in 1-dimensional vectors d_1, d_2 and d_3. Vectors d_1 and d_2 account for changes when volume features are taken into account. d_1 has values when the deformable model is near to the noisy skull, and it is zero when it is far from the noisy skull. d_2 stores the contribution of the Gradient Vector Flow when a control point is far from the noisy volume. Vector d_3 stores displacements originated by the shape term. The deformation function used to update the positions

Algorithm 1 Template Deformation

Require: Skull template properly initialised
  while (stop condition not meet) **do**
    Variable initialisation :
    $i = d_j(x_i) = d_j(y_i) = d_j(z_i) \leftarrow 0$;
    $\{(i,j) | \ 1 \leq j \leq 3;\ 0 \leq i \leq Number\ of\ Control\ Points\}$
    for *each control point* i **do**
      calculate intersection of the ray from CP_i (at the skull template)
      to the noisy volume in its normal direction within a range
      if (intersection exists) **then**
        calculate $d_1(x_i), d_1(y_i), d_1(z_i)$ in direction of the intersecting point
        set: $d_2(x_i) = d_2(y_i) = d_2(z_i) \leftarrow 0$
      else
        set: $d_1(x_i) = d_1(y_i) = d_1(z_i) \leftarrow 0$
        calculate $d_2(x_i), d_2(y_i), d_2(z_i)$ from the GVF direction
      end if
    end for
    Set $d_3(x_i), d_3(y_i), d_3(z_i) \leftarrow 0$
    Calculate Shape energy vector d_3
    Deform the model using RBF-TPS using $CP_i + d_3$
    Evaluate the stop condition
  end while

Figure 2: *Template deformation algorithm.*

of the control points is based on a Radial basis function with a Thin-Plate-Spline base [CBC*]:

$$f_k(\mathbf{x}) = p_m(\mathbf{x}) + \sum_{i=1}^{n} \ _i \ _i(\| \mathbf{x} - \mathbf{x}_i \|) \qquad (14)$$

The value of the function $_i$ depends only on the distance of the point $\mathbf{x}$ to each of the control points $\mathbf{x}_i$ (The $\mathbf{x}_i$ points are called centers). The weights of the basis functions $_i$ are found by placing the centres back into $f_k(\mathbf{x})$ and solving the resulting set of linear equations. The polynomial term p_m is included to allow a certain degree of polynomial precision. The MRI dataset used in this work was created at the University of Sheffield [†]. It consists of a set of scans of the head and neck of 60 subjects, and their corresponding biographical information: age, sex, ancestral affiliation (ethnicity). Additionally, information of whether the individual's relatives were also volunteering was also recorded. Each volume contains 200 gray-scaled 256 x 256 pixel sagittal images. The format of each image is 16 bit per pixel raw data with information of approximately the aorta level and up. Using our extraction algorithm, a database of 60 skull-face models were generated and the 40 best models were used in the CFR system described in the next section. Figure 3 shows an example of the skull and face models generated with the extraction processes. The face models used are produced by using Marching Cubes algorithm [LC87]. The face meshes are registered with respect to a common mesh using

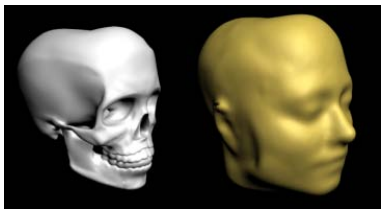

Figure 3: *The resulting surface models for the skull and face of the first individual of the database.*

the same Robust Point Matching algorithm [CR] previously mentioned in the skull extraction section [‡].

3. Craniofacial Reconstruction System

Using skull-face information obtained from MRI, the novelty of the CFR system presented is that it is the first system build based exclusively on this type of data. The skull-face relation provides an implicit and more extensive way to guide the reconstruction process, and as shown in the CFR system, can be used to produce reconstruction results based on statistical data of the whole face (rather than the discrete landmark based methods [KHS03]). The craniofacial reconstruction system consists of three main elements: Skull Examination, Template Construction and Face Construction. In the first stage, an input skull is analysed and a set of main features extracted. Combining these features with information about the skull-face relationship, and a spatial deformable technique, this system creates possible face estimations for the input skull. The anthropometric information is provided by the database of head models presented in section 2. The reconstruction technique is based on a template deformation approach. A head template (skull-face pair) is created by combining several heads models from the database. These models are selected with similar features to the unknown subject. The age, sex, body constitution, PCA coefficients, and geometric properties of the unknown skull are used as selection conditions. The head template is deformed to fit the unknown skull to produce a face estimation. The deformation approach used is based on a Radial basis function approach with a thin plate spline base (see equation 14). The use of spatial deformation allows the facial tissues (skull, muscle, etc.) to be dealt with as a single component, freeing the procedure from the problem of placing and interpreting anthropometric landmarks associated with soft tissue depth tables [MC96, VVMN00]. Facial soft tissues should change in response to the changes in the skull, and therefore the face is not merely a mask depending on a small number of soft tissue depth points, as is the case, for example, in [CVG*06].

[†] The dataset was obtained thanks to the collaboration with Dr. Martin Evison from the Forensic Pathology Department (now at working at the Centre for Forensic Science and Medicine, University of Toronto) and Dr. Iain Wilkinson from the Academic Unit of Radiology from the University of Sheffield

[‡] This registration is also used to smooth the models. The difference between the marching cubes and the registered smoothed facial versions is on average less than 0.2mm

The k reference head (skull-face) models whose facial models are F_r^i $(i = 1 \ldots k)$, are combined for producing a face estimation are contained in the set H_b:

$$\begin{aligned} \mathbf{H}_b &= \{\mathbf{H}_r^1, \mathbf{H}_r^2 \ldots \mathbf{H}_r^k\} = \{\{S_r^1, F_r^1\}, \\ &\quad \{S_r^2, F_r^2\}, \ldots \{S_r^k, F_r^k\}\} \end{aligned} \tag{15}$$

For example, if the criterion is the minimum procrustes distance d between the skull shapes [DM98], the set $\mathbf{H}_b$ of selected head models is defined as:

$$\begin{aligned} \mathbf{H}_b &= \{\{S_r^i, F_r^i\} \mid i \in \{j \mid d(S_r^j, S_u) \\ &< \ , j \in \{1 \ldots n\}\}\} \end{aligned} \tag{16}$$

where n is the number of elements of the database, S_r^j is a reference skull model of the j^{th} database entry, and $\|\mathbf{H}_b\| = k$ for some threshold value accounting for a limit for the difference in procrustes distance d between models S_r^j and S_u. Using a leave-one-out strategy [VCL*06], a skull $S_u \in H_u$ will simulate the skull whose face will be reconstructed and its skin layer F_u will then be used to evaluate the results.

The process of face estimation is shown schematically in figure 4. In this stage, a deformation function f will be calculated between S_u and each of the reference skulls $S_r^j \in \mathbf{H}_b$:

$$f_j(S_r^j) = S_u \tag{17}$$

This mapping function f_j will be used to estimate a deformed face $\hat{F}_u^j$ for each of the j reference models, by applying this function to the corresponding reference face F_r^j as follows:

$$\hat{F}_u^j = f_j(F_r^j) \tag{18}$$

The resulting reconstructed face $\hat{F}_u$ is then the average of the $\hat{F}_u^j$ elements:

$$\hat{F}_u = \sum_{j=1}^{k} \frac{\hat{F}_u^j}{k} \tag{19}$$

The functions f_j are based on the Radial Basis Function deformation approach [CBC*]. The set of matching control points between the source and target models are obtained directly from the relation between the vertices of both models (they share a common vertex structure because they were originated with the skull template deformations scheme presented in section 2.4).

4. Results

The results of the CFR system are obtained by means of a comparison between the reconstructed face and the real face surface evaluated by using a surface to surface metric (The average difference between both surfaces). The system was tested with 27 different combination of biological and geometrical features. Figure 6 shows the criteria used for generating the craniofacial reconstructions. Negated attributes mean that different features were used to select models from the database (e.g. $\overline{Sex}$ means that the models used were of the opposite genre to the sex of the unknown skull). Negated criteria were included to quantify the impact of choosing the wrong features in the CFR system and to corroborate that positive criteria give better reconstruction results than negative criteria. In the case of age, BMI, Procustes Distance and PCA, the data is grouped in classes and for calculating the negated features, most dissimilar classes are used. For example in the case of the age, the subjects are separated into 5 groups (see table 1): 20-35, 26-30, 31-40, 41-50 and 51-70, labelled age1-5. For calculating $\overline{age}$ the following criteria was used: select age_4 models if the unknown skull belongs to age_0, age_1 or age_2 group. Use age_0 otherwise. A detailed description of each criterion can be consulted in [Sal10]. Figure 5 shows 6 facial reconstructions for the skull of subject 18 of the UOS dataset. In this case, the third row shows the best face reconstruction of the group i.e. the one with lowest average distance between surfaces) and it was obtained using models of individuals of the same sex and similar age as the unknown skull. Figure 7 shows skull 18 of the UOS dataset and figures 8 and 9 show the best reconstruction generated. In the graph of figure 10 the average distances between the real and the reconstructed faces sorted by criteria used are shown [§]. Criteria t_0 to t_{14} show that, when adding information to the CFR system about the unknown skull, the CFR system implemented gives results with less than 2.0 mm between the reconstructed and the real faces. Using negative criteria, the average error was not greater than 2.5mm. In general, as expected, positive criteria produced better results that negative criteria. Using a leave-one-out strategy, 850 facial reconstructions were generated using different criteria based on feature matching using the sex, age, body build and geometric features of the input skull. The results obtained were comparable to other techniques using evaluation criteria based on surface to surface distance metrics obtaining average distances of less than 2.0 mm.

5. Conclusions

We have presented a novel approach to extracting skulls from MRI datasets, based on a probabilistic approach for guiding the evolution of a 3D deformable template. By incorporating shape knowledge of the skull, our approach is able to cope with uncertainty problems in regions where it is difficult to establish skull boundaries. This property is useful to overcome the strong homogeneity restrictions exposed in the methods presented in section 2.1 (most of them based only on one intensity criteria to separate skull elements). The

[§] In this work, due to data confidentiality, we present a limited number of models. However, data plotted in figure 9 summarises the general results obtained per reconstruction criteria for all the experiments

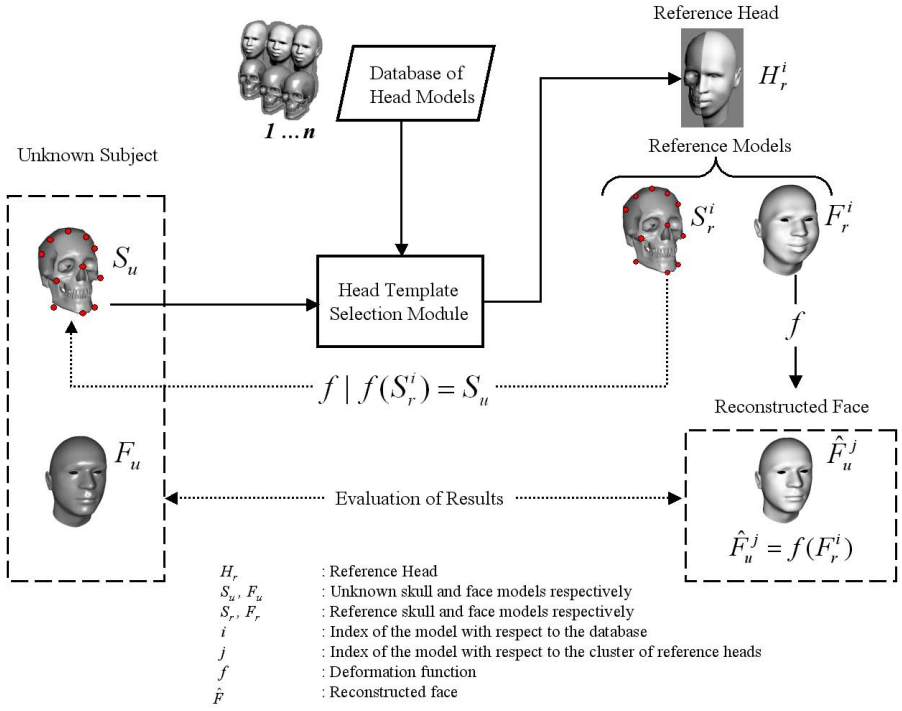

Figure 4: *The template selection process.*

extraction process, in conjunction wth the use of the marching cubes algorithm [LC87] for face extraction from the MRI dataset, has been used to create a database of skullface models for use in a craniofacial reconstruction (CFR) system. The CFR results obtained are comparable to other CFR approaches, and offer the advantage of more consistent reconstructions, with each stage being easier to control and evaluate, removing the subjectivity of artist-driven approaches. In addition, since MRI datasets can be readily obtained, the database could be easily extended. **Acknowledgements**. M. Salas acknowledges CONACyT Mexico for the scholarship support for this research and also thanks Dr. Martin Evison and Dr. Iain Wilkinson for providing the MRI datasets for conducting this research.

References

[BA] BULU H., ALPKOCAK A.: Comparison of 3d segmentation algorithms for medical imaging. In *Proc. CBMS 2007*, pp. 269–274.

[CBC*] CARR J., BEATSON R., CHERRIE J., FRIGHT T. M. W., MCCALLUM B., EVANS T.: Reconstruction and representation of 3D objects with radial basis functions. In *Proc. SIGGRAPH 2001*, pp. 67–76.

[CR] CHUI H., RANGARAJAN A.: A New Algorithm for Non-Rigid Point Matching. In *Proc. CVPR 2000*, vol. 2, pp. 40–51.

[CSB07] CLAYDEN J., STORKEY A., BASTIN M.: A probabilistic model-based approach to consistent white matter tract segmentation. *Medical Imaging 26*, 11 (November 2007), 1555–1561.

[CVG*06] CLAES P., VANDERMEULEN D., GREEF S. D., WILLEMS G., SUETENS P.: Craniofacial reconstruction using a combined statistical model of face shape and soft tissue depths: Methodology and validation. *Forensic Sci. Int. 159 (Suppl1)* (2006), 147–158.

[DM98] DRYDEN I., MARDIA K.: *Statistical Shape Analysis*. John Wiley, July 1998.

[DSL05] DOGDAS B., SHATTUCK D., LEAHY R.: *Segmentation of skull and scalp in 3-D human MRI using mathematical morphology*, vol. 26-4. Wiley-Liss, 2005, ch. Human Brain Mapping, pp. 273–285.

[Evi00] EVISON M.: Modeling Age, Obesity, and Etnicity in a Computerized 3-D Facial Reconstruction. In *9th Biennial Meeting of the International Association for Craniofacial Identificaction* (FBI, Washington DC, July 2000).

[GAMK*08] GHADIMI S., ABRISHAMI-MOGHADDAM H., KAZEMI K., GREBE R., GOUNDRY-JOUET C., WALLOIS F.: Segmentation of scalp and skull in neonatal MR images using probabilistic atlas and level set method. *Engineering in Medicine and Biology Society, EMBS* (Aug 2008), 3060–3063.

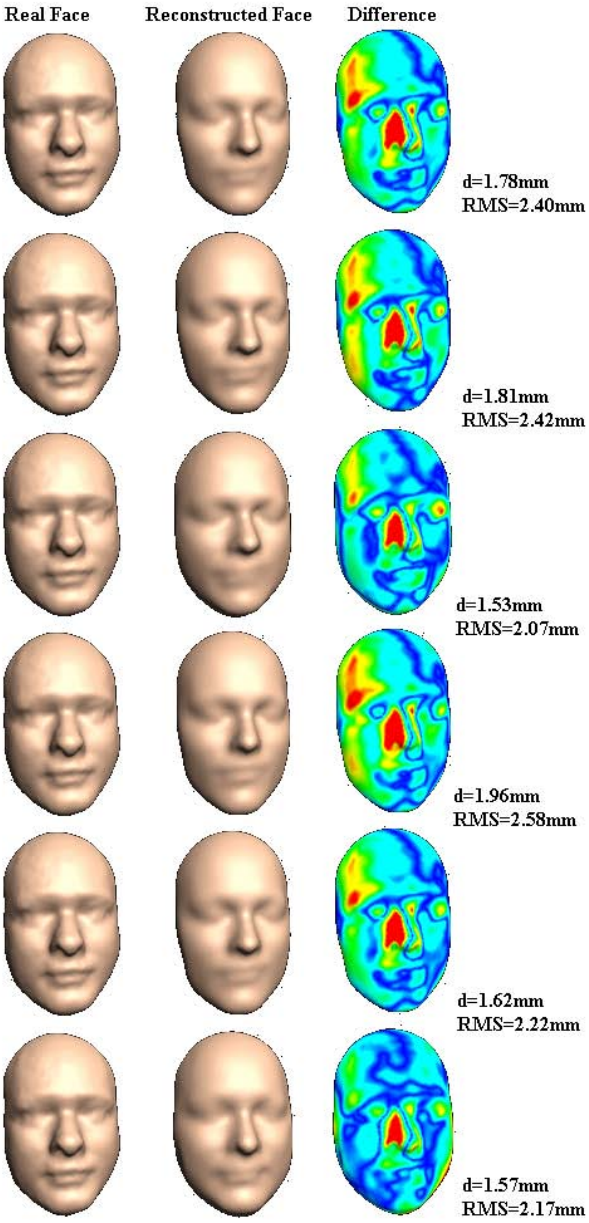

Figure 5: *An example of five results of the CFR system for the skull of the subject 18 of the UOS dataset. Each row represents a criteria for the reconstruction (t0-t5)*

Test	Feature criteria	Test	Feature criteria
t_0	All the database	...	*Continuation ...*
t_1	*Sex*	t_{14}	$\overline{PCA}$
t_2	*Age* band	t_{15}	$\overline{Proc}$
t_3	*PCA* band	t_{16}	$\overline{BMI}$
t_4	*Proc* distance	t_{17}	$\overline{Sex}$ & $\overline{Age}$
t_5	*BMI* band	t_{18}	$\overline{Sex}$ & $\overline{Age}$ & *PCA*
t_6	*Sex* & *Age*	t_{19}	$\overline{Sex}$ & $\overline{Age}$ & *Proc*
t_7	*Sex* & *Age* & *PCA*	t_{20}	$\overline{Sex}$ & $\overline{Age}$ & $\overline{PCA}$
t_8	*Sex* & *Age* & *Proc*	t_{21}	$\overline{Sex}$ & $\overline{Age}$ & $\overline{Proc}$
t_9	*Sex* & *Age* & *BMI*	t_{22}	$\overline{Sex}$ & $\overline{Age}$ & $\overline{BMI}$
t_{10}	*Sex* & *Age* & *PCA* & *BMI*	t_{23}	$\overline{Sex}$ & $\overline{Age}$ & *PCA* & $\overline{BMI}$
t_{11}	*Sex* & *Age* & *Proc* & *BMI*	t_{24}	$\overline{Sex}$ & $\overline{Age}$ & *Proc* & $\overline{BMI}$
t_{12}	$\overline{Sex}$	t_{25}	$\overline{Sex}$ & $\overline{Age}$ & $\overline{PCA}$ & $\overline{BMI}$
t_{13}	$\overline{Age}$	t_{26}	$\overline{Sex}$ & $\overline{Age}$ & $\overline{Proc}$ & $\overline{BMI}$

Figure 6: *Criteria used for the facial reconstructions*

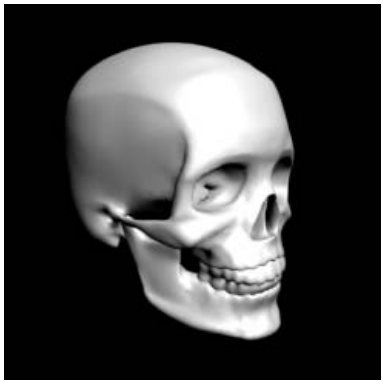

Figure 7: *Skull model 18 of the UOS dataset.*

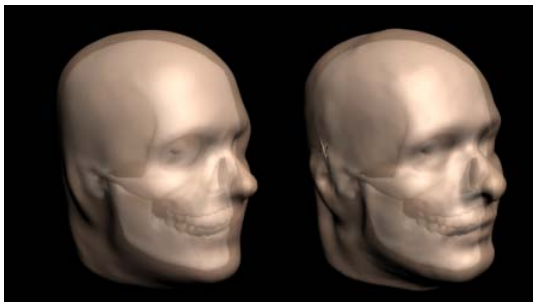

Figure 8: *An example of the best reconstruction for skull model 18 of the UOS dataset. The figure shows the reconstructed face on the base skull (left) and the real head model of the skull (right). The best reconstruction score was obtained applying criterion t6 based on sex and age.*

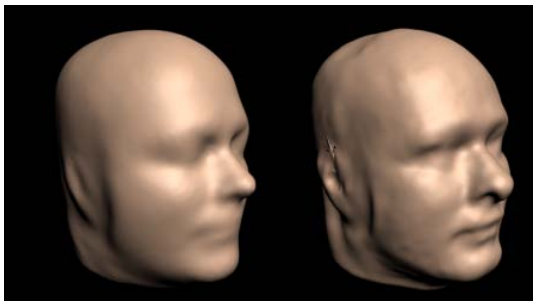

Figure 9: *Facial surface reconstructed of the example in figure 8. Again, the reconstructed face (left) and original face (right). The results corresponds to criterion t6 (Sex & Age) with* $\bar{d} = 1.42$ *mm and RMS* $= 1.98$ *mm.*

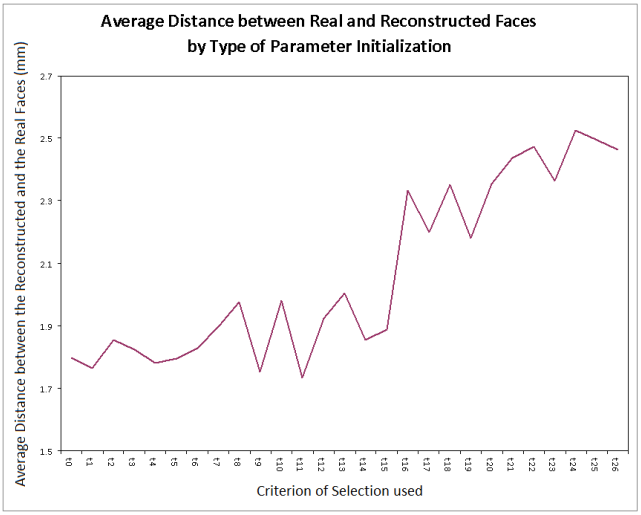

Figure 10: *Average distances of reconstruction for criteria presented in figure 6*

[HED*97] HEINOEN T., ESKOLA H., DASTIDAR P., LAARNE P., MALMIVUO J.: Segmentation of T1 MR scans for reconstruction of resistive head models. *Computer Methods and Programs in Biomedicine 54* (1997), 173–181.

[KBCL99] KENDALL D., BARDEN D., CARNE T., LE H.: *Shape and Shape Theory*. John Wiley and Sons, 1999.

[KHS03] KÄHLER K., HABER J., SEIDEL H.: Reanimating the Dead: Reconstruction of Expressive Faces from Skull Data. In *ACM Transactions on Graphics* (San Diego, USA, July 2003), of ACM SIGGRAPH 2003 P., (Ed.), pp. 27–31.

[LC87] LORENSEN W., CLINE H.: Marching Cubes: a high resolution 3D surface reconstruction algorithm. In *Computer Graphics* (1987), vol. 21-4, Proc. SIGGRAPH, pp. 163–169.

[LFB98] LAIDLAW D., FLEISCHER K., BARR A.: Partial-volume bayesian classification of material mixtures in mr volume data using voxel histograms. *IEEE Transactions on Medical Imaging 17* (1998), 100–112.

[LJZ03] LU Y., JIANG T., ZANG Y.: Region growing method for the analysis of functional MRI data. *NeuroImage 20* (2003), 455–465.

[LLA*08] LÜTHI M., LERCH A., ALBRECHT T., KROL Z., VETTER T.: A hierarchical multi-resolution approach for model-based skull-segmentation in mri volumes. *Conference Proceedings 3D-Physiological Human* (December 2008), 1–8.

[LMVS03] LEEMPUT K., MAES F., VANDERMEULEN D., SUETENS P.: A Unifying Framework for Partial Volume Segmentation of Brain MR Images. *IEEE Transactions on Medical Imaging 22*, 1 (2003), 105–119.

[MC96] MICHAEL S., CHEN M.: The 3D Reconstruction of Facial Features Using Volume Distortion. In *Proceedings 14th Eurographics UK Conference* (March 1996), pp. 297–305.

[MMB06] MANG A., MÜLLER J., BUZUG T. M.: A multi-modality computer-aided framework towards postmortem identification. *Journal of Computing and Information Technology (CIT) 14*, 1 (2006), 7–19.

[RBH*00] RIFAI H., BLOCH I., HUTCHINSON S., J.W., GARNERO L.: Segmentation of the skull in mri volumes using deformable model and taking the partial volume effect into account. *Medical Image Analysis 4*, 3 (2000), 219 – 233.

[Sal10] SALAS M.: *Extracting Skull-Face Models from MRI datasets for use in Craniofacial Reconstruction*. PhD thesis, University of Sheffield, March 2010.

[SHJ*07] SHAN Z., HUA C., JI Q., PARRA C., YING X., KRASIN M., MERCHANT T., KUN L., REDDICK W.: A Knowledge-guided Active Model of Skull Segmentation on T1-weighted MR images. In *SPIE Medical Imaging* (March 2007), vol. 6512.

[Sma96] SMALL G.: *The Statistical Theory of Shape*. Springer Series in Statistics, 1996.

[VCL*06] VANDERMEULEN D., CLAES P., LOECKX D., DE GREEF S., WILLEMS G., SUETENS P.: Computerized craniofacial reconstruction using ct-derived implicit surface representations. *Forensic Science International 259 (Suppl)* (2006), 164–174.

[VVMN00] VANEZIS P., VANEZIS M., MCCOMBE G., NIBLETT T.: Facial reconstruction using 3-D computer graphics. *Forensic Science International 108*, 2 (February 2000), 81–95.

[XP00] XU C., PRINCE J.: *Handbook of Medical Imaging*. Academic Press, September 2000.